

Supporting information for

Synthesis of chiral functionalized UiO-66-NH₂@SiO₂ and use of its domain-limiting effect for separating small enantiomers

Chunqiang Liu,^{ab} Kaijun Quan,^{*a} Hui Li,^a Xiaofeng Shi,^c Jia Chen,^a and Hongdeng Qiu^{*ab}

^a CAS Key Laboratory of Chemistry of Northwestern Plant Resources and Key Laboratory for Natural Medicine of Gansu Province, Lanzhou Institute of Chemical Physics, Chinese Academy of Sciences, Lanzhou 730000, China

^b University of Chinese Academy of Sciences, Beijing 100049, China

^c Institute of Materia Medica, Gansu Provincial Cancer Hospital, Lanzhou 730050, China

* E-mail: quankj@licp.cas.cn (K. Quan); hdqiu@licp.cas.cn (H. Qiu)

1. Chemicals and materials

Silica (3 μm) was donated from Shanxi Intelligent Micro Technology Company, Limited (IMTECH). Ultra-pure water is obtained by Milli-Q ultra-pure water purification equipment in our laboratory. Chromatographic reagents such as N-hexane, isopropanol and methanol are provided by Merida reagents. A stainless steel empty column (150 mm long × 4.6 mm i.d.) was purchased from Tianjin three dimensional chromatography instrument Co. Ltd. (Tianjin, China). 2-Aminoterephthalic acid (98%), zirconium chloride (98%), 3-aminopropyltrimethoxysilane (APTES) (97%), and (+)-diacetyl-L-tartaric anhydride (DATA) (97%) were purchased from Shanghai Aladdin Biochemical Technology Co.,Ltd. Succinic anhydride (99%) was purchased from Saen Chemical Technology (Shanghai) Co., Ltd. Dibenzoyl-(+)-tartaric acid (DBTA)(99%) was purchased from Beijing Aoke Biotechnology Co., Ltd. N-hydroxysuccinimide (NHS)(97%) was purchased from Shanghai Kefeng Chemical Reagent Co., Ltd. 1-ethyl-(3-dimethylaminopropyl) carbodiimide hydrochloride (EDC) (98.5%) was purchased from Shanghai Macklin Biochemical Co., Ltd.

2. Apparatus and characterizations

All compounds were tested by LC-15C system, binary pump and ultraviolet detector (SHIMADZU, Japan). Binary pump was used to control the proportion of mobile phase online. IFS-120HR Fourier Transform Infrared

Spectrometer (FT-IR, Bruker Company, Germany); Milli-Q ultra-pure water purification equipment (Milli-pore, Billerica Company, USA); Column loading system is American Haskel gas driven pump 95,551U model; The element analysis results were determined by Vario EL III element analyzer (Hanau, Germany); Thermal analysis (TGA) was measured by 449F3 synchronous thermal analyzer (Netzsch, Germany); Scanning electron microscope (JSM-5600LV, SEM, JOEL, Japan). N₂ adsorption and desorption surface areas were measured at 77K by the BET technique on a Micromeritics ASPS 2010 analyzer (USA).

3. *Synthesis of carboxylic-functionalized silica microspheres (SiO₂-COOH)*

The carboxylated silica microspheres were prepared by three steps based on the research of Liu et al.¹ with small modification. First, for the activation of silica, silica microspheres (2.0 g) were soaked in 38% hydrochloric acid solution overnight, the product were washed with ultrapure water and ethanol to neutral and then vacuum dried 24h at 60 °C. Second, for the amination of silica (SiO₂-NH₂), activated silica microspheres (2.0 g), anhydrous toluene (50 mL) and 3-aminopropyltrimethoxysilane (APTES, 1mL) were added into a 100 mL flask. After reacting at 80°C for 24h, the product were washed with methanol and ethanol. Then the SiO₂-NH₂ were obtained by vacuum dried 24h at 60 °C. Third, for the carboxylated silica (SiO₂-COOH), amion-functionalized silica microspheres (1.0 g), succinic anhydride (2.0 g) and N,N-dimethylformamide (45 mL) were added into a 100 mL flask. After reacting at 45°C for 12h, the product were washed with ethanol. Then the SiO₂-COOH were obtained by vacuum dried 24h at 60 °C.

4. *Synthesis of UiO-66-NH₂*

UiO-66-NH₂ was synthesized according to previous work² with small modification. Briefly, 2-aminoterephthaic acid (1 mmol, 0.181 g), ZrCl₄ (1 mmol, 0.233 g) and acetic acid (100 mmol, 6 mL) were mixed with DMF (50 mL) in a teflon-lined bomb. Then the teflon-lined bomb was placed in an oven at 120 °C for 24h. After cooling down to room temperature, the final light yellow product was collected by centrifuging and washed with DMF and MeOH several times. Finally, the UiO-66-NH₂ particles were obtained by vacuum dried 24h at 60 °C.

5. *Synthesis of UiO-66-DATA*

The preparation of UiO-66-DATA: UiO-66-NH₂ (0.14 g), (+)-diacetyl-L-tartaric anhydride (0.13 g) and DMF (30 mL) were added into a 100 mL flask. After reacting at 45°C for 12h, the product were washed with DMF and

ethanol. Then the UiO-66-DATA were obtained by vacuum dried 24h at 60 °C.

6. *Synthesis of UiO-66-NH₂@SiO₂*

UiO-66-NH₂@SiO₂ was prepared by a simple "one-pot" method, which was different from the previous preparation methods.^{3, 4} Briefly, SiO₂-COOH (1.62 mmol, 0.3 g), ZrCl₄ (1.62mmol, 0.384 g), H₂BDC (1.62mmol, 0.3 g), acetic acid (162mmol, 9.264 mL) and DMF (30 mL) were added into a 100 mL flask, after reacting at 120°C for 24h, the product were washed with DMF and MeOH several times. Finally, the UiO-66-NH₂@SiO₂ particles were obtained by vacuum dried 24h at 60 °C.

7. *Synthesis of UiO-66-DATA@SiO₂*

The preparation of UiO-66-DATA@SiO₂ was simple. Briefly, UiO-66-NH₂@SiO₂ (1.8 g), (+)-diacetyl-L-tartaric anhydride (1.5 g) and DMF (45 mL) were added into a 100 mL flask. After reacting at 45°C for 12h, the product were washed with DMF and ethanol. Then the UiO-66-DATA@SiO₂ were obtained by vacuum dried 24h at 60 °C.

8. *Synthesis of UiO-66-DBTA@SiO₂*

The preparation of UiO-66-DBTA@SiO₂: First, Dibenzoyl-(+)-tartaric acid (DBTA) (1.074 g) and 1-ethyl-(3-dimethylaminopropyl)carbodiimide hydrochloride (EDC) (0.573 g) were added to DMF (50 mL). Ultrasonic oscillation treatment was performed for 10 min, followed by stirring for 20 min, and then UiO-66-NH₂@SiO₂ (2.4 g) and N-hydroxysuccinimide (NHS) (0.345 g) were added. After reacting at 60°C for 24h, the product were washed with DMF and ethanol, respectively. Then the UiO-66-DBTA@SiO₂ were obtained by vacuum dried 24h at 60 °C.

9. *Synthesis of DATA@SiO₂*

The preparation of DATA@SiO₂: SiO₂-NH₂ was prepared in the same way as above. SiO₂-NH₂ (2.4 g), (+)-diacetyl-L-tartaric anhydride (2.0 g) and DMF (50 mL) were added into a 100 mL flask. After reacting at 45°C for 12h, the product were washed with DMF and ethanol. Then the (Ac-L-Ta)@SiO₂ were obtained by vacuum dried 24h at 60 °C.

10. *Synthesis of DBTA@SiO₂*

The preparation of DBTA@SiO₂: SiO₂-NH₂ was prepared in the same way as above. First, Dibenzoyl-(+)-

tartaric acid (DBTA) (1.074 g) and 1-ethyl-(3-dimethylaminopropyl)carbodiimide hydrochloride (EDC) (0.573 g) were added to DMF (50 mL). Ultrasonic oscillation treatment was performed for 10 min, followed by stirring for 20 min, and then SiO₂-NH₂ (2.4 g) and N-hydroxysuccinimide (NHS) (0.345 g) were added. After reacting at 60°C for 24h, the product were washed with DMF and ethanol, respectively. Then the DBTA@SiO₂ were obtained by vacuum dried 24h at 60 °C.

11. Preparation of packed UiO-66-DATA@SiO₂ and UiO-66-DBTA@SiO₂ column

The chiral stationary phase, Chir-UiO-66-NH₂@SiO₂ was packed into 150 mm × 4.6 mm i.d. stainless steel columns according to a slurry packing procedure. UiO-66-DATA@SiO₂ and UiO-66-DBTA@SiO₂ core-shell spheres (2.4 g) were dispersed in a vessel with MeOH (50 mL) with the ultrasound for 10 min. Then the dispersion was packed into empty stainless steel colume under 40 Mpa using MeOH as the propulsion solvent. The prepared chiral column was balanced with MeOH at a flow rate of 0.1 mL min⁻¹ for 3 h before chromatographic testing.

12. Calculation of chromatographic parameters

The retention factor (k), separation factor (α) and resolution value (Rs) were calculated according to Eqs. S1-4, respectively.⁵

$$k_1 = \frac{t_1 - t_0}{t_0} \quad (1)$$

$$k_2 = \frac{t_2 - t_0}{t_0} \quad (2)$$

$$\alpha = \frac{k_2}{k_1} \quad (3)$$

$$Rs = 1.18 \times \frac{t_2 - t_1}{W_{1/2(1)} + W_{1/2(2)}} \quad (4)$$

In the above equations, ‘ t ’ was the retention time of the peak (t₁ for peak 1 and t₂ for peak 2), ‘ t₀ ’ was dead time, ‘ k ’ was the retention factors of the peak (k₁ for peak 1 and k₂ for peak 2,) ‘ α ’ was the separation factors, ‘ Rs ’ was the resolution, and W_{1/2} was the half-peak width of the chromatographic peak (W_{1/2(1)} for peak1 and W_{1/2(2)} for peak 2).

13. The feasibility of using chiral tartaric acid derivatives as chirality source

Upon the post-modification of UiO-66-NH₂ with DATA, the position of the original PXRD characteristic peak of UiO-66-NH₂ remained unchanged for UiO-66-DATA, the intensity of the peak changed slightly, and the crystalline state and morphology remained intact. Meanwhile, fluorescence spectroscopy of UiO-66-DATA showed that the maximum emission wavelength remained unchanged and the fluorescence intensity values were enhanced upon the introduction of DATA. Therefore, the feasibility of using chiral tartaric acid derivatives as a source of chirality for the post-modification of UiO-66-NH₂ were demonstrated (**Fig. S1**).

14. The Fourier-transform infrared (FT-IR) spectra of SiO₂-NH₂ and SiO₂-COOH

In the Fourier-transform infrared (FT-IR) spectra of SiO₂-NH₂, the intensities of the signals at 3375 cm⁻¹ and 2935 cm⁻¹, corresponding to N-H and C-H groups, respectively, were greater for SiO₂-NH₂ than SiO₂, which proved that the condensation reaction between APTES and Si-OH had occurred. The successful preparation of SiO₂-COOH was also confirmed by the appearance of characteristic signals at 1725 cm⁻¹ and 1563 cm⁻¹ for the C=O and -CO-NH groups, respectively (**Fig. S3**).

15. Fluorescent chiral recognition experiment of UiO-66-DATA

In order to investigate the differences in the interaction between amino acid molecules and stationary phases, valine and serine were analyzed, specifically looking at the difference in chiral recognition of the different enantiomers by UiO-66-DATA. By investigating the effect of enantiomers on the fluorescence properties of UiO-66-DATA, the interaction between the enantiomers and UiO-66-DATA were analyzed. The difference between the effect of d-valine and that of l-valine on the fluorescence intensity of UiO-66-DATA was found to be small, while the difference between the effect of d-serine and that of l-serine on the fluorescence intensity of UiO-66-DATA was greater, proving that the two enantiomers of serine formed different interactions with the UiO-66-DATA and showed a better chiral recognition difference (**Fig. S10**).

16. Repeatability and mechanical stability of column A and column B

The reproducibility of the column **A** and column **B** were investigated by using phenylethylamine and mandelonitrile as the analytes, respectively, with five consecutive injections. The results showed that the relative standard deviation (RSD) of the retention times of phenylethanolamine on column **A** and mandelonitrile on column **B** are 0.3%-0.2% and 0.4%-0.6% (n=5), respectively. None of the chiral

selectivity were changed, confirming that column A and column B have good separation reproducibility and stability. In addition, methanol is used as the mobile phase with flow rate ranges from 0.2 mL/min to 0.7 mL/min. The back pressure of the column A and column B shows a good linearity with the change of flow rate ($R^2 > 0.99$), which indicated column A and column B has good mechanical stability for high performance liquid chromatography separation (**Fig. S12**).

17. Synthetic reproducibility of column A and column B

The synthetic reproducibility was evaluated by preparing three different batches of A and B stationary phase packing with mandelonitrile as the analytical target. The three different batches of stationary phase packing also have homogeneous morphology in the SEM images (**Fig. S13**). And the chiral selectivity also remained stable, therefore, good synthetic reproducibility of UiO-66-DATA@SiO₂ (column A) and UiO-66-DBTA@SiO₂ (column B) were demonstrated (**Fig. S14**).

18. Effect of the injection volume on HPLC enantiomer separation

The enantiomer mandelonitrile was used to evaluate the effect of injection volume on the column A and B. The retention time did not change with the increase of injection volume, and the chiral selectivity remained stable. The peak height of the column showed good linearity with the injection volume ($R^2 > 0.99$), which indicated that the column has good quantitative analysis ability (**Fig. S15**).

19. Effect of mobile phase on HPLC enantiomer separation

The enantiomer mandelonitrile was used to evaluate the effect of mobile phase on the column A. With the increasing of the content of n-hexane in mobile phase, the retention (k_2), separation factor (α) and resolution value (R_s) tended to increase. This phenomenon was also reflected in alanine and serine. This may be attributed to the existence of hydrogen bonding interaction and coordination action between the stationary phase and the guest molecule in the system of n-hexane-isopropanol. The increase of isopropanol content weakened the hydrogen bonding interaction and coordination, which leads to the weakening of the retention of guest molecule (**Fig. S16**).

20. Effect of flow rate on HPLC enantiomer separation

The enantiomer mandelonitrile was used to evaluate the effect of flow rate on the column A. The retention factor (k) and separation factor (α) did not change significantly. The reason of the increase of the resolution value (R_s) was that the higher flow rate reduced the peak broadening caused by longitudinal diffusion, so the flow rate did not significantly affect the retention time and chiral selectivity (**Fig. S17**).

Table S1. Elemental analysis of SiO₂-NH₂, SiO₂-COOH, UiO-66-NH₂@SiO₂, UiO-66-DATA@SiO₂ and UiO-66-DBTA@SiO₂.

Modified silica	Elemental contents %		
	N	C	H
SiO ₂ -NH ₂	1.63	5.08	1.228
SiO ₂ -COOH	1.30	8.29	1.291
UiO-66-NH ₂ @SiO ₂	2.10	15.82	2.809
UiO-66-DATA@SiO ₂	1.54	16.03	1.859
UiO-66-DBTA@SiO ₂	1.80	17.42	2.285

Table S2. Separation of racemates on the column **A** and column **B**.

Racemates	Mobile phase (N-hexane / isopropanol)		Retention factor (k)		Separation factor (α)		Resolution value (Rs)				
	A	B	A	B	A	B	A	B	C	D	E
phenylethylamine	90:10	50:50	0.85	1.25	1.57	2.16	2.65	1.09	--	--	--
mandelonitrile	90:10	50:50	0.92	0.65	1.89	1.64	2.85	1.11	1.06	0.98	0.44
alanine	20:80	0:100	1.2	1.39	1.75	1.84	1.06	1.35	--	--	--
serine	20:80	0:100	0.96	1.14	1.62	1.70	1.22	0.81	--	--	--
methionine	20:80	0:100	1.33	1.65	1.86	2.07	1.30	1.32	--	--	--
arginine	20:80	0:100	1.39	1.52	1.92	2.02	1.45	1.44	--	--	--
histidine	20:80	0:100	1.30	1.80	1.84	2.13	1.26	1.56	--	--	--
asparagine	10:90	0:100	0.83	1.18	1.57	1.73	0.92	0.78	--	--	--
cystine	10:90	0:100	0.92	1.25	1.66	1.83	1.22	1.02	--	--	--
threonine	10:90	0:100	0.94	1.44	1.64	1.96	1.06	1.10	--	--	--
lysine	10:90	0:100	0.97	1.41	1.65	1.94	1.07	1.09	--	--	--
phenylalanine	--	50:50	--	0.58	--	1.49	--	1.33	--	--	--

-- : not separated.

Table S3. Three-dimensional sizes of the analyzed enantiomers.

Enantiomers	Three-dimensional sizes (Å)
phenylethylamine	9.219 × 6.592 × 5.279
mandelonitrile	9.326 × 6.963 × 4.515
alanine	7.381 × 6.165 × 5.066
serine	7.536 × 6.203 × 5.081
methionine	10.083 × 6.016 × 5.965
arginine	11.923 × 6.368 × 5.745
histidine	10.834 × 5.957 × 5.182
asparagine	8.487 × 6.184 × 5.594
cystine	13.795 × 6.582 × 5.706
threonine	7.652 × 6.386 × 5.621
lysine	10.870 × 6.093 × 5.613
phenylalanine	11.300 × 6.893 × 5.264
carvedilol	17.254 × 12.404 × 8.343
labetalol	18.157 × 8.666 × 6.578

The above data were provided by Chemdraw 3D and Jerkwin.

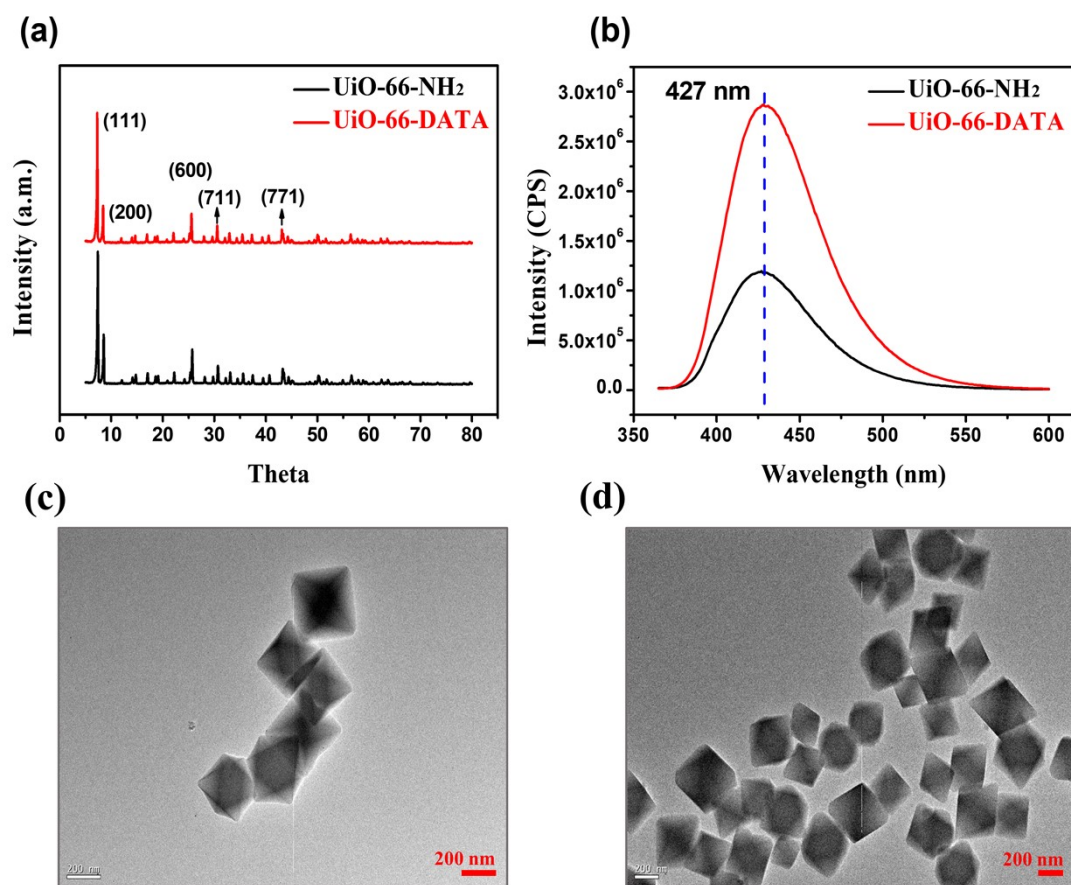


Fig. S1 (a) PXRD patterns of the prepared UiO-66-NH₂ and UiO-66-DATA; (b) Fluorescence spectra of the prepared UiO-66-NH₂ and UiO-66-DATA; (c) TEM image of UiO-66-NH₂ and (d) TEM image of UiO-66-DATA.

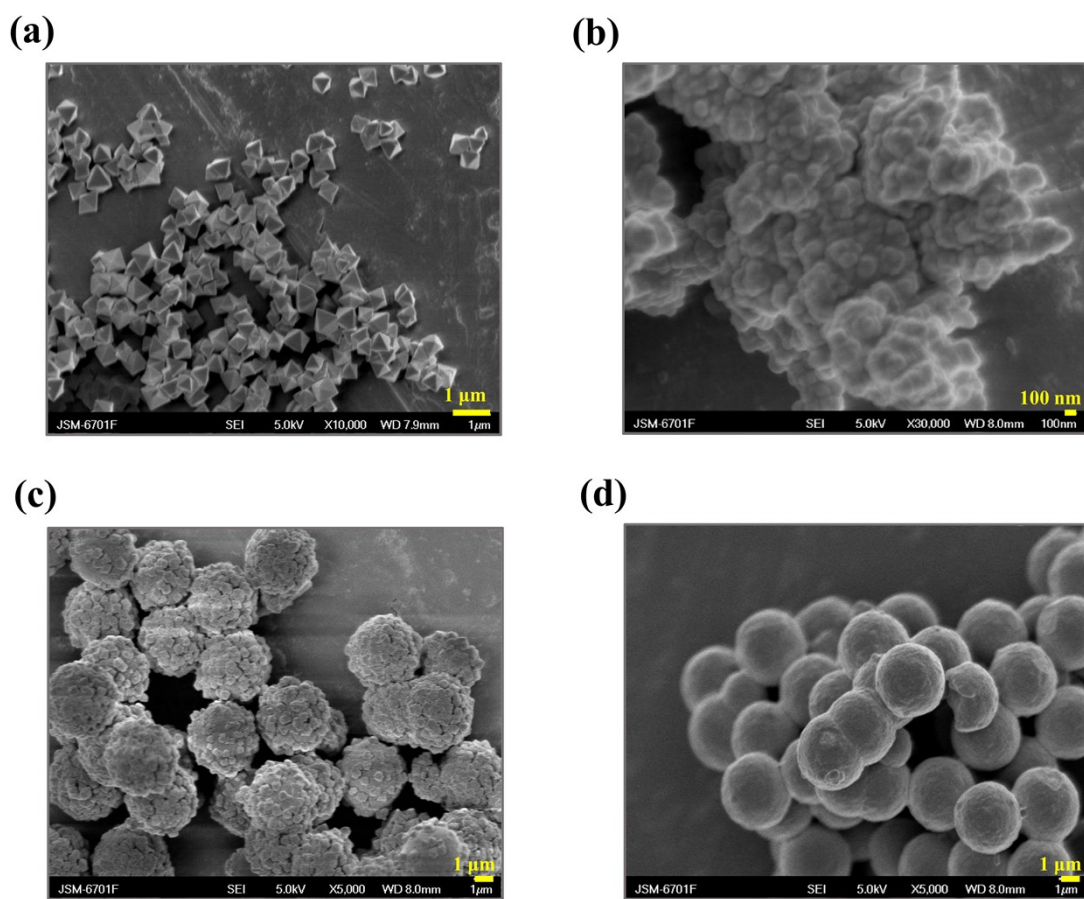


Fig. S2 SEM image of (a) UiO-66-NH₂ (acetic acid added); (b) UiO-66-NH₂ (no acetic acid added); (c) UiO-66-NH₂@SiO₂ (acetic acid added) and (d) UiO-66-NH₂@SiO₂ (no acetic acid added).

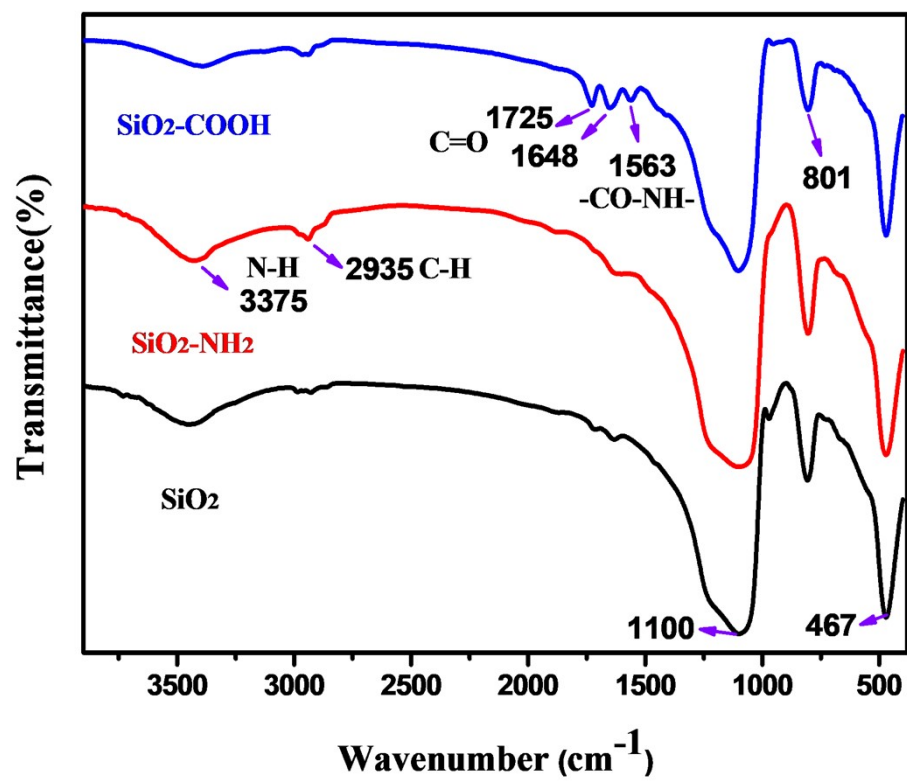


Fig. S3 (a) FT-IR patterns of SiO₂, SiO₂-NH₂ and SiO₂-COOH.

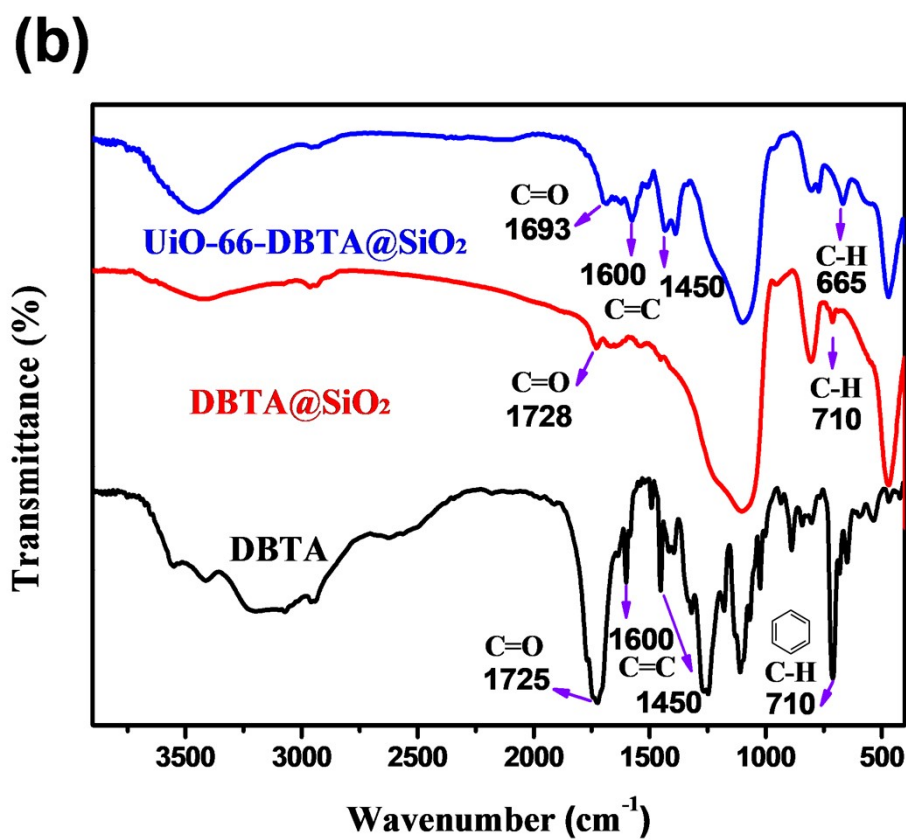
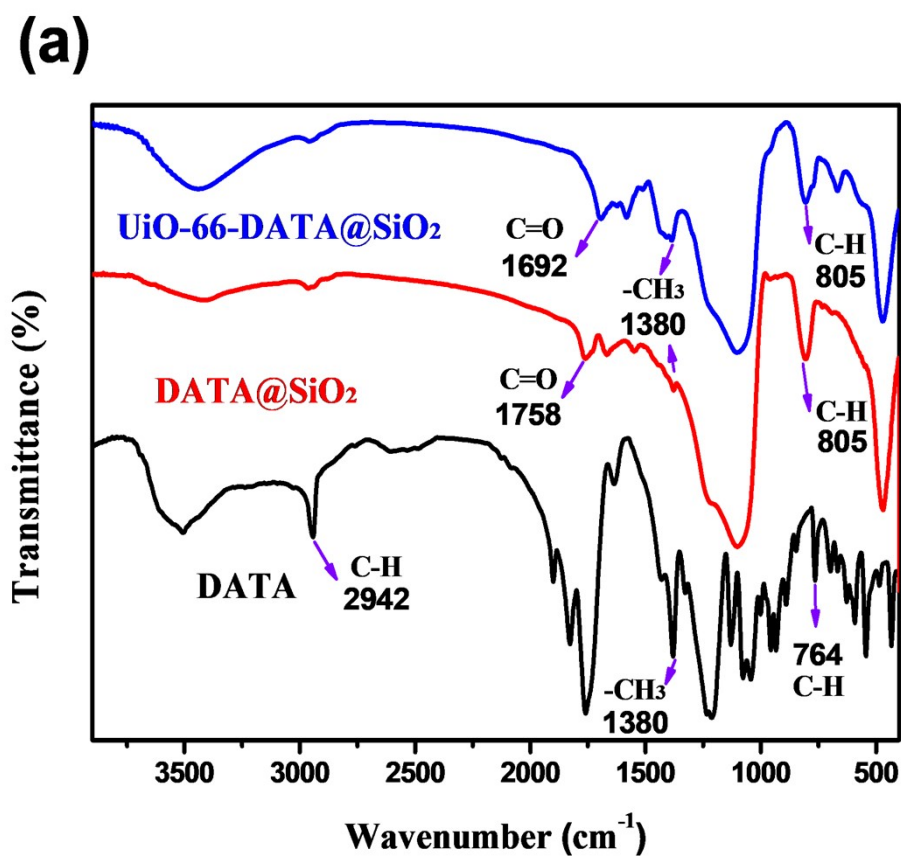


Fig S4. FT-IR spectra of (a) DATA, DATA@SiO₂, UiO-66-DATA@SiO₂ and (b) DBTA, DBTA@SiO₂, UiO-66-DBTA@SiO₂

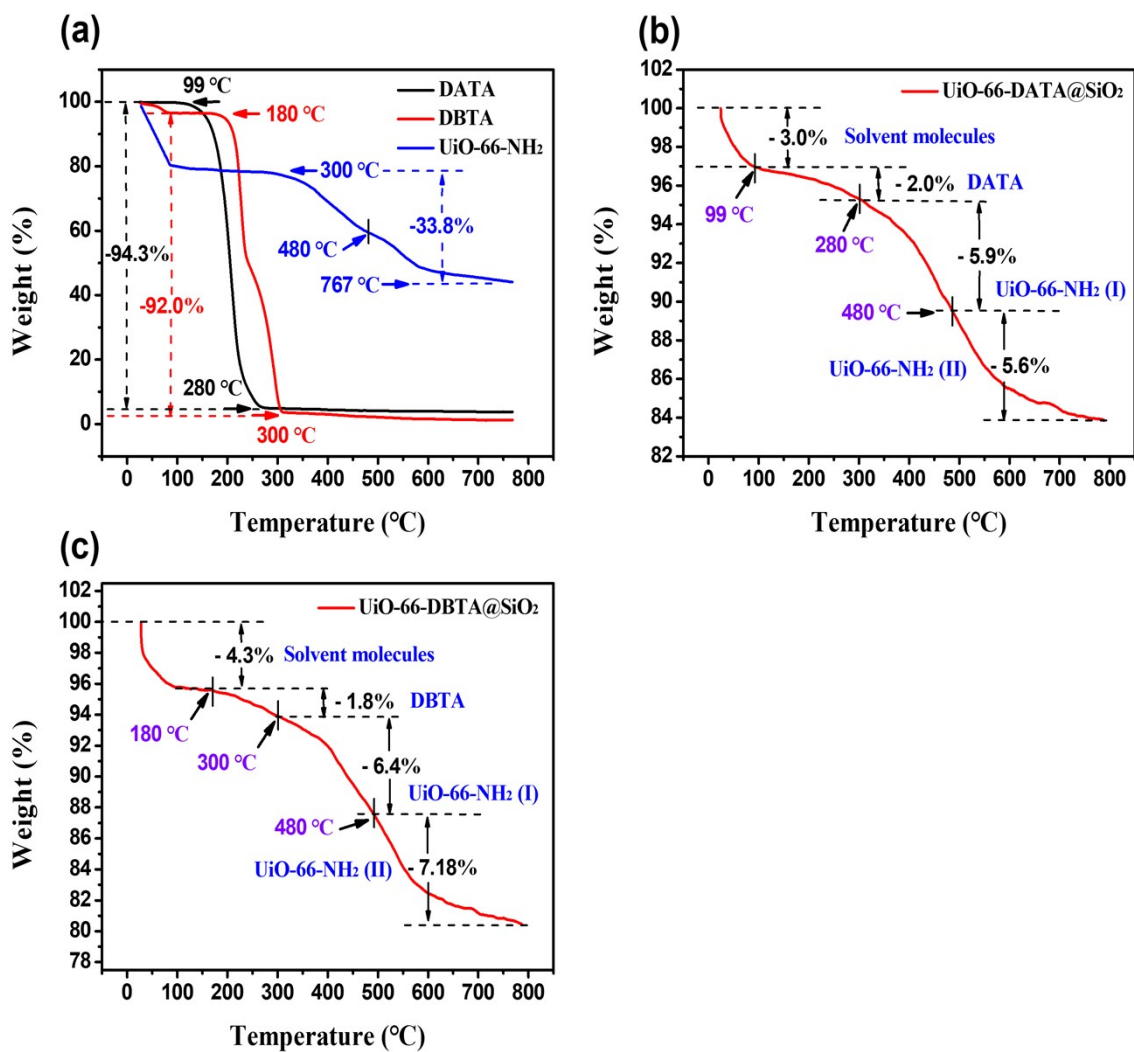


Fig. S5 TGA curves of (a) DATA, DBTA and UiO-66-NH₂ (b) UiO-66-DATA@SiO₂ and (c) UiO-66-DATA@SiO₂.

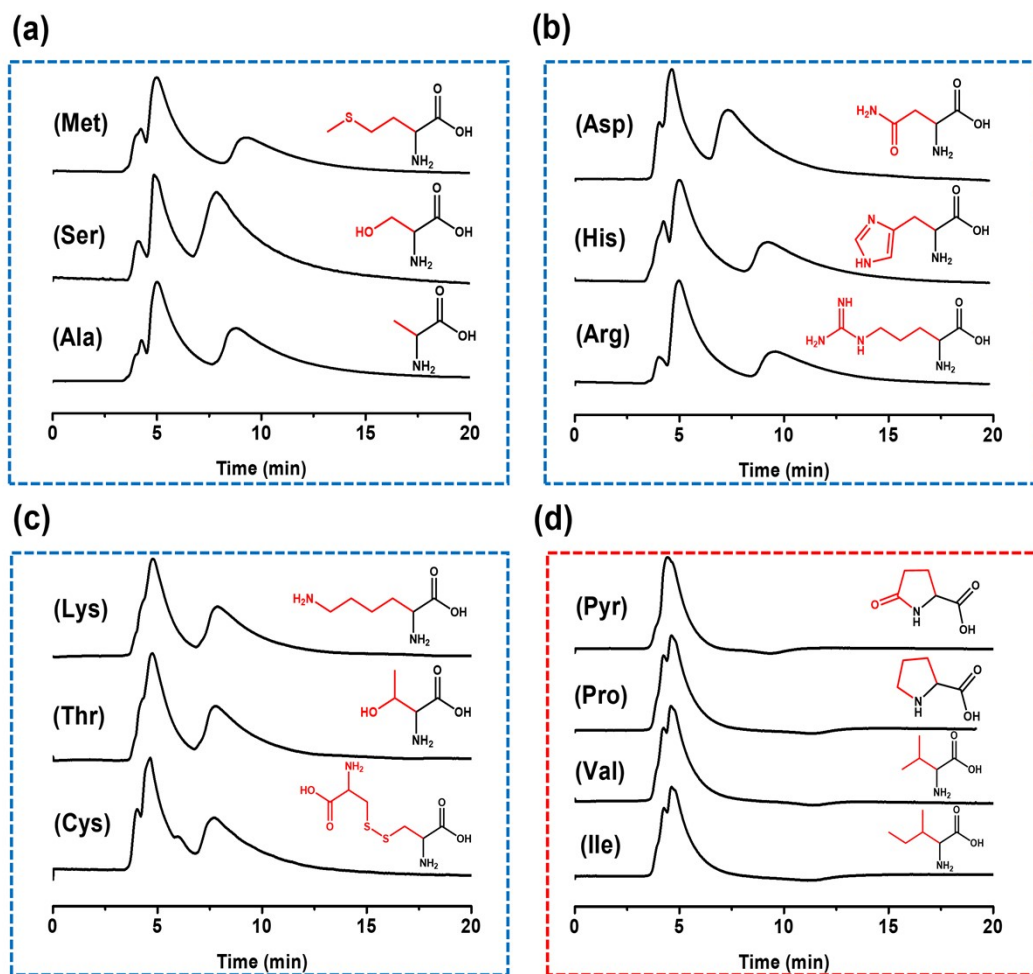


Fig. S6 HPLC chromatograms of thirteen amino acid on the UiO-66-DATA@SiO₂ (column A) at 25 °C. Experimental conditions: mobile phase, N-hexane:isopropanol, (a) 20:80, 0.5 mL/min; (b) arginine and histidine: 20:80, 0.5 mL/min; Asparagine: 10:90, 0.5 mL/min; (c) 10:90, 0.5 mL/min; (d) 10:90, 0.5 mL/min. The signal was monitored with a UV detector at 254 nm.

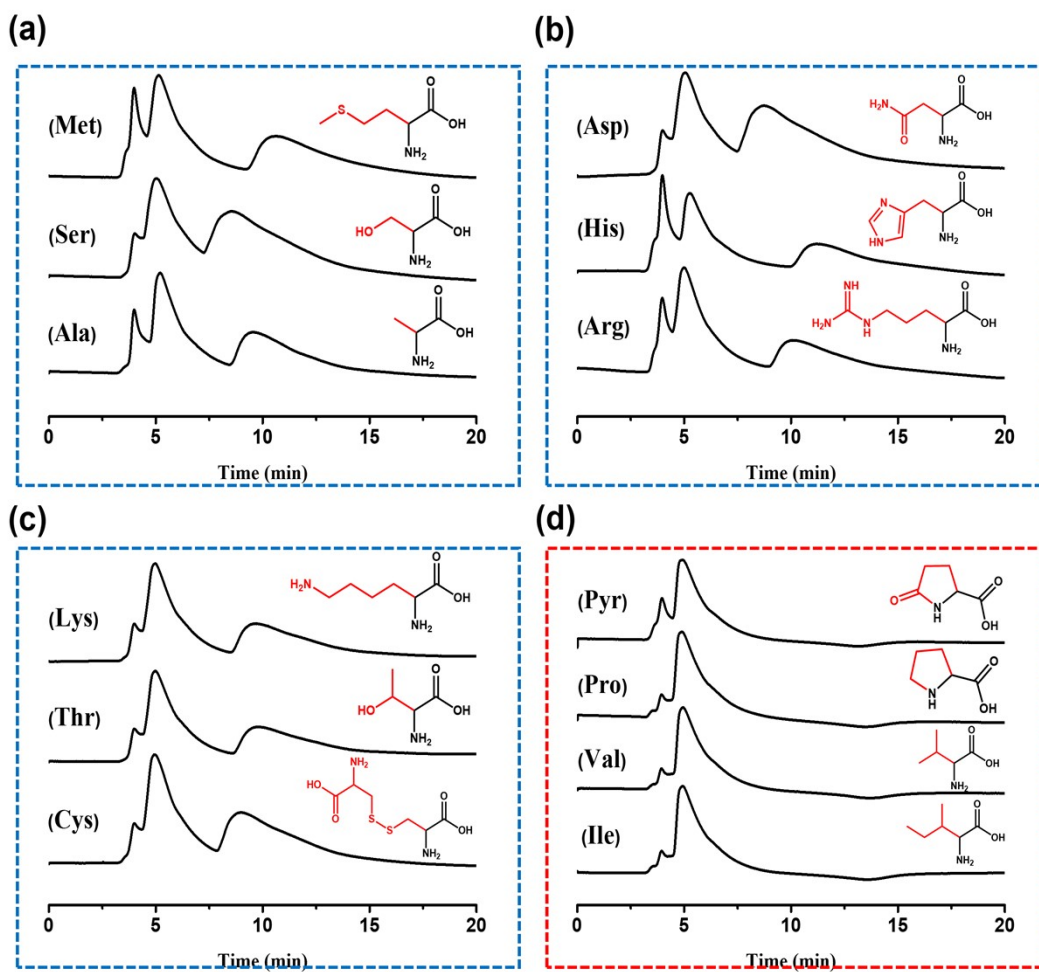


Fig. S7 HPLC chromatograms of thirteen amino acid on the UiO-66-DBTA@SiO₂ (column **B**) at 25 °C. Experimental conditions: mobile phase, N-hexane:isopropanol; 10:90, 0.5 mL/min. The signal was monitored with a UV detector at 254nm.

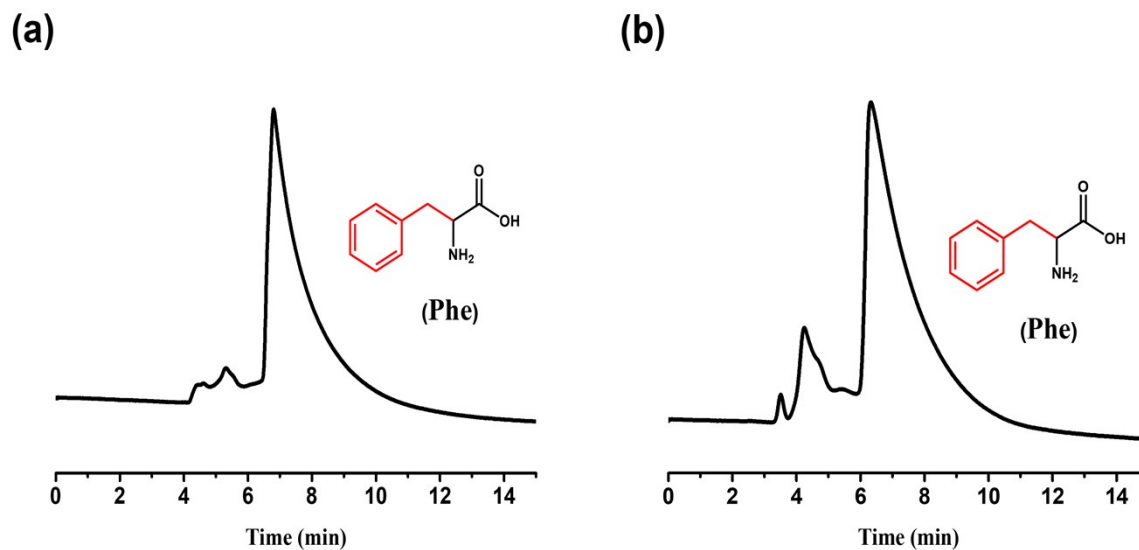


Fig. S8 HPLC chromatograms of phenylalanine on the (a) UiO-66-DATA@SiO₂ (column A) and (b) UiO-66-DBTA@SiO₂ (column B) at 25 °C. Experimental conditions: mobile phase, N-hexane:isopropanol; 50:50, 0.5 mL/min.. The signal was monitored with a UV detector at 254nm.

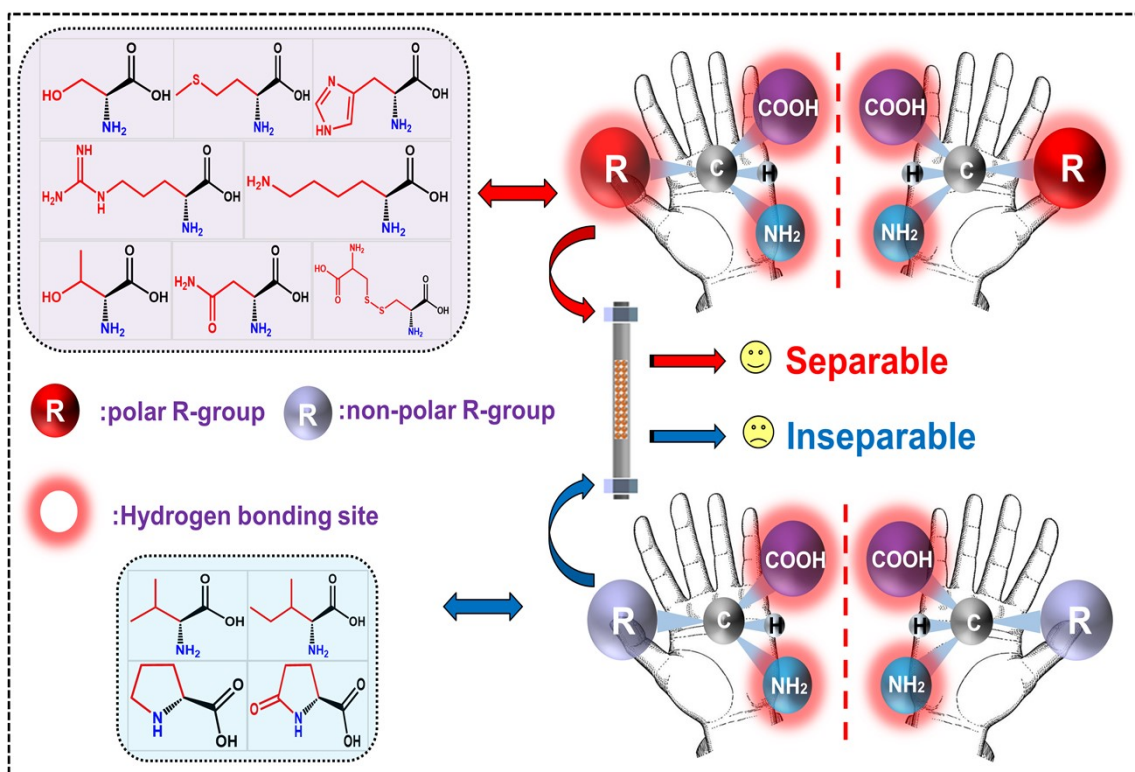


Fig. S9 Diagram of the separation law of fourteen α -amino acids on UiO-66-DATA@SiO₂ (column A) and UiO-66-DBTA@SiO₂ (column B).

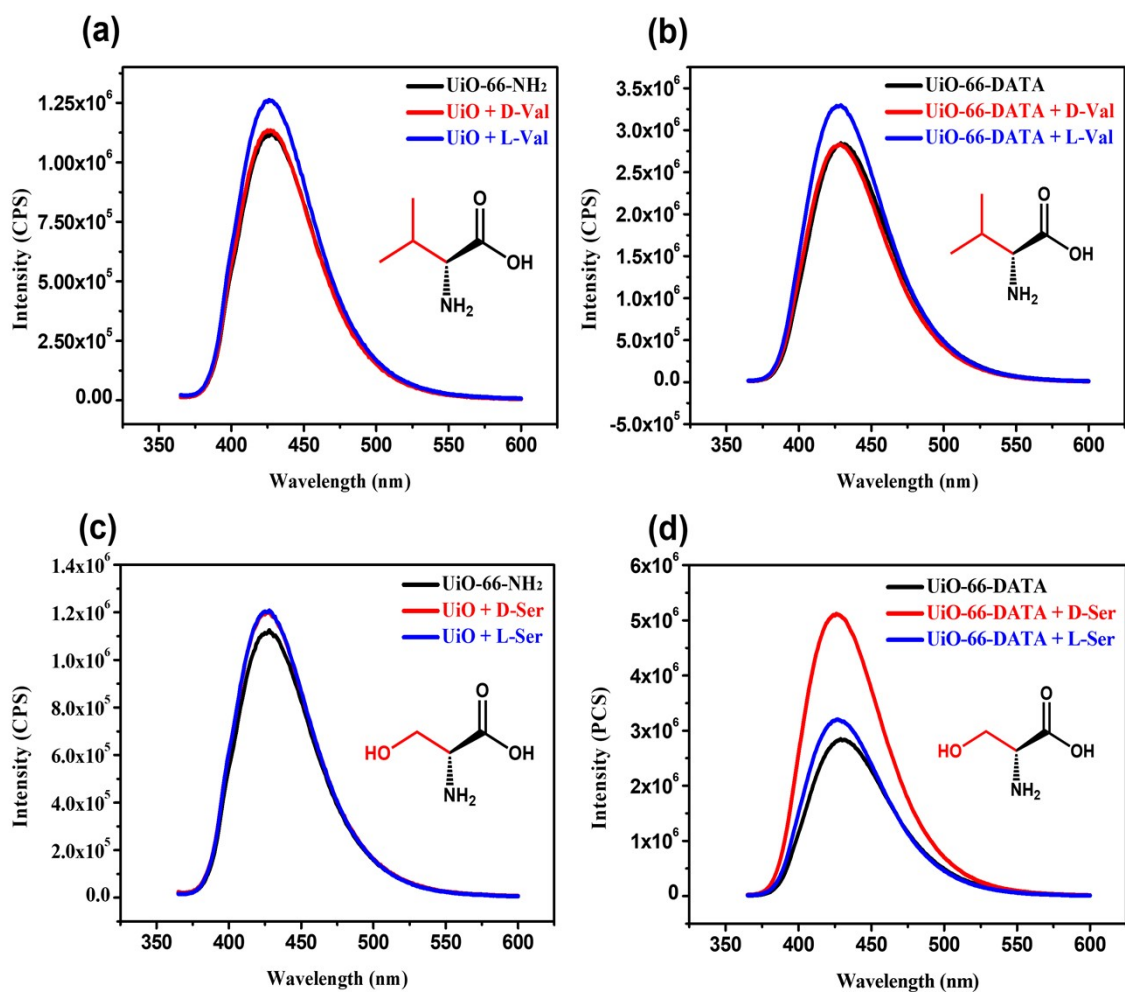


Fig. S10 Fluorescence spectra of chiral recognition: (a) D/L-valine recognized by UiO-66-NH₂; (b) D/L-valine recognized by UiO-66-DATA; (c) D/L-serine recognized by UiO-66-NH₂; (d) D/L-serine recognized by UiO-66-DATA.

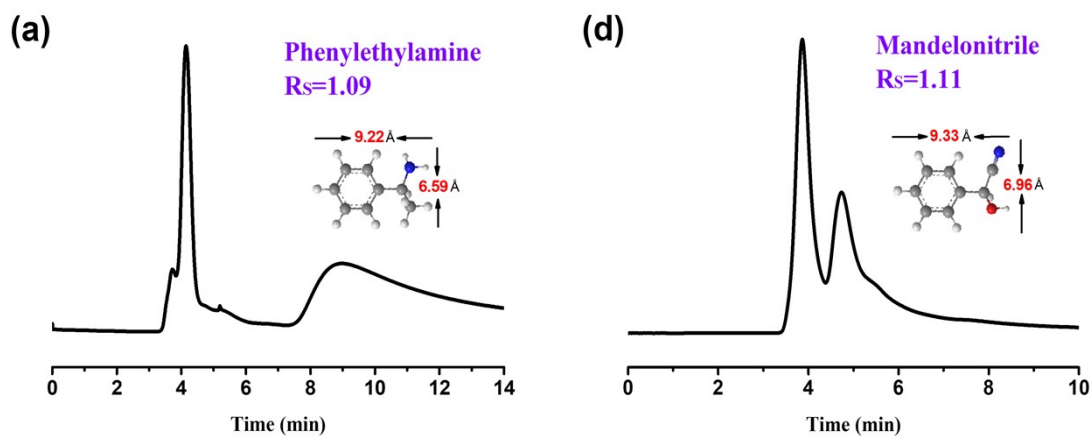


Fig. S11 HPLC chromatograms of (a) phenylethylamine and (b) mandelonitrile on UiO-66-DBTA@SiO₂ (column **B**) at 25 °C. Experimental conditions: mobile phase, N-hexane:isopropanol; 50:50, 0.5 mL/min.. The signal was monitored with a UV detector at 254nm.

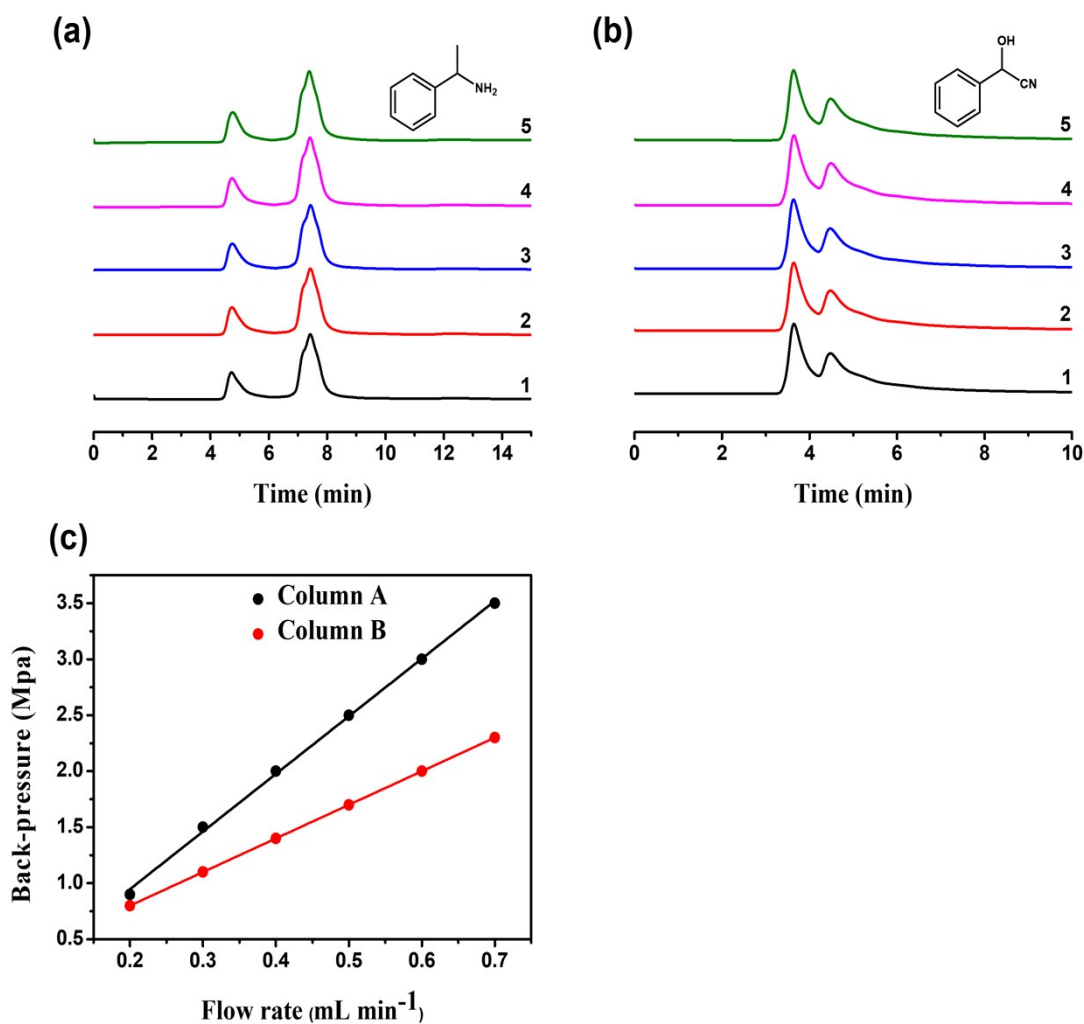


Fig. S12 (a) HPLC chromatograms obtained on the UiO-66-DATA@SiO₂ (column **A**) for the separation of phenylethylamine by repeated injection for five times. (b) HPLC chromatograms obtained on the UiO-66-DBTA@SiO₂ (column **B**) for the separation of mandelonitrile by repeated injection for five times. The signal was monitored with a UV detector at 254nm. (c) Back pressure against flow rate for column **A** and column **B**. Experimental conditions: mobile phase, pure MeOH; flow rate, 0.2-0.7 mL min⁻¹.

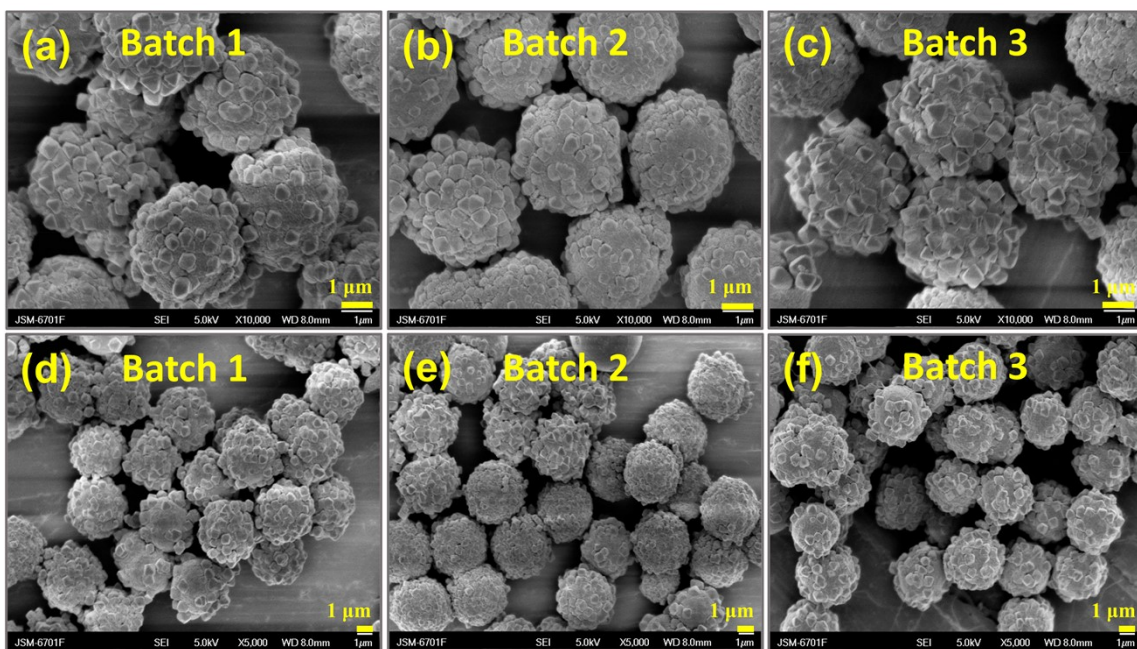


Fig. S13 SEM images of three different batches of (a-c) UiO-66-DATA@SiO₂ and (d-f) UiO-66-DBTA@SiO₂.

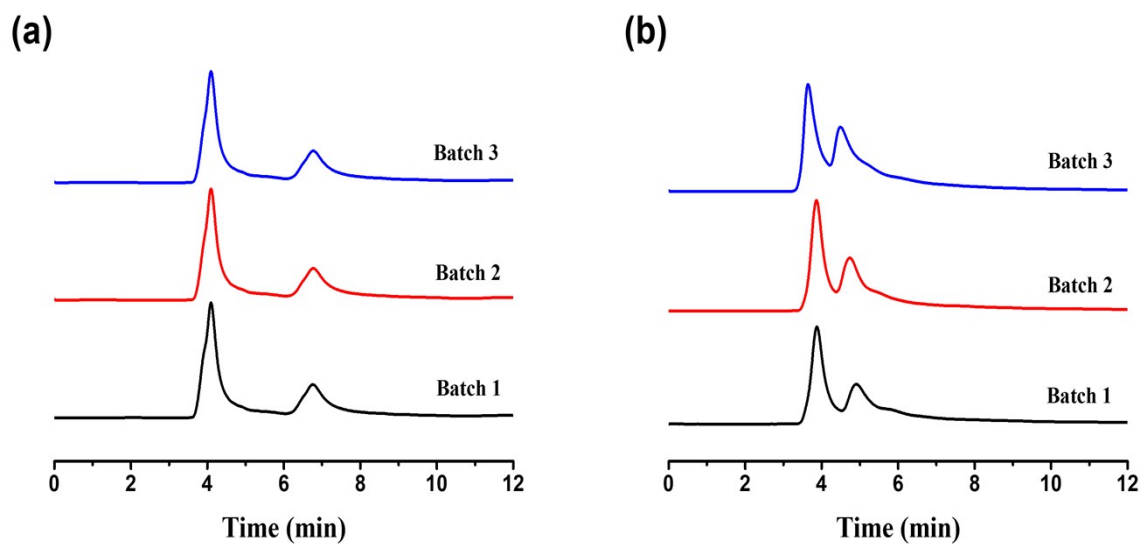


Fig. S14 Reproducibility of three different batches of (a) UiO-66-DATA@SiO₂ (column A) and (b) UiO-66-D BTA@SiO₂ (column B). Analyte: mandelonitrile. Experimental conditions: (a) N-hexane:isopropanol = 80:20, 0.5 mL min⁻¹ (b) N-hexane:isopropanol = 50:50, 0.5 mL min⁻¹. The signal was monitored with a UV detector at 254nm.

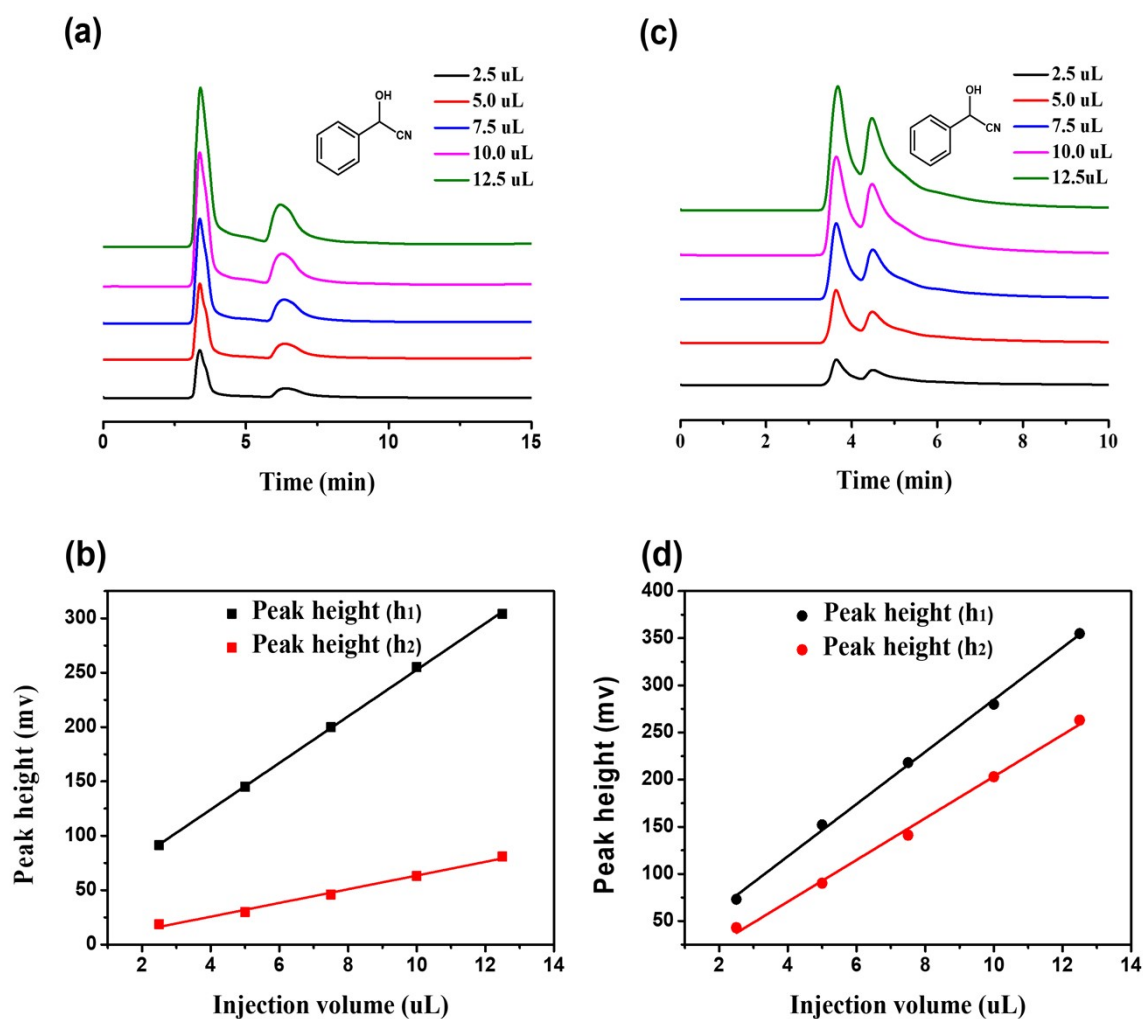


Fig. S15 (a) HPLC chromatograms of mandelonitrile on UiO-66-DATA@SiO₂ (column **A**) using different injection volume (2.5, 5.0, 7.5, 10.0, and 12.5 uL) at 25 °C. (b) Peak height against injection volume for column **A**. (c) HPLC chromatograms of mandelonitrile on UiO-66-DBTA@SiO₂ (column **B**) using different injection volume (2.5, 5.0, 7.5, 10.0, and 12.5 uL) at 25 °C. (d) Peak height against injection volume for column **B**. Experimental conditions: (a) mobile phase, N-hexane:isopropanol = 90:10 ; flow rate, 0.6 mL min⁻¹. (c) mobile phase, N-hexane:isopropanol = 50:50; 0.5 mL min⁻¹. The signal was monitored with a UV detector at 254 nm.

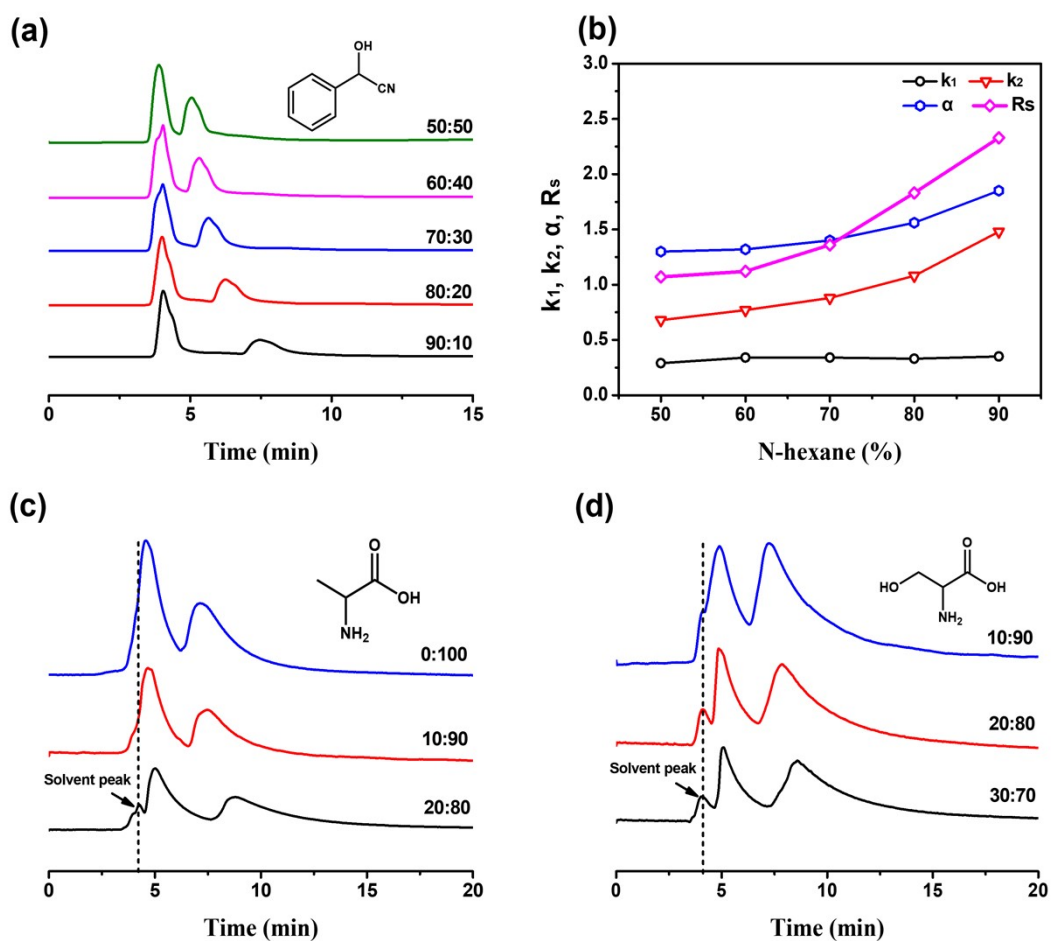


Fig. S16 (a) HPLC chromatograms of mandelonitrile on UiO-66-DATA@SiO₂ (column A) with different solvent systems and (b) Variation trend of k_1 , k_2 , α and R_s at 25 °C; (c) HPLC chromatograms of alanine on the column A; (d) HPLC chromatograms of serine on the column A. Experimental conditions: mobile phase, N-hexane:isopropanol. The signal was monitored with a UV detector at 254nm.

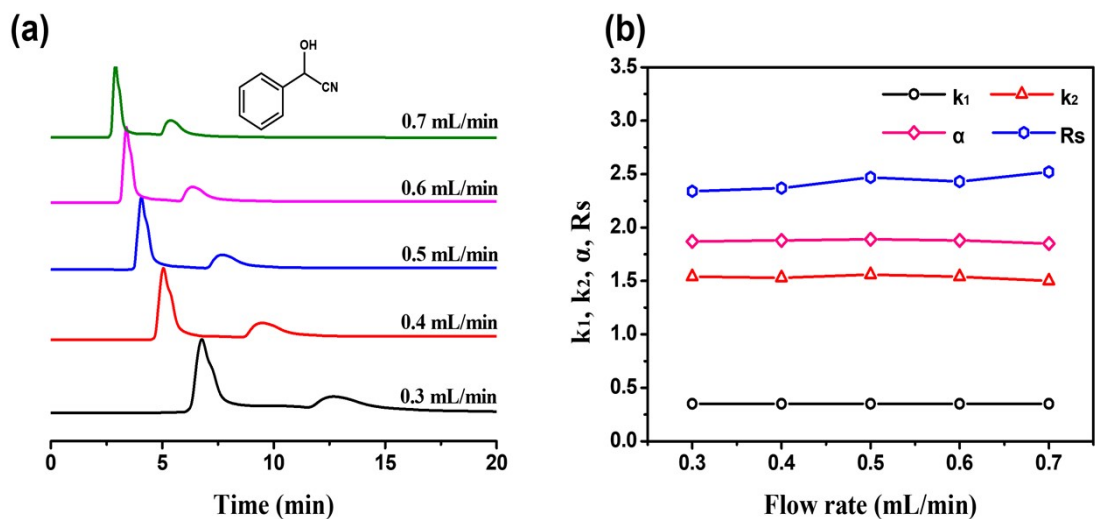


Fig. S17 HPLC chromatograms of mandelonitrile on UiO-66-DATA@SiO₂ (column A) with different flow rate (0.3, 0.4, 0.5, 0.6, and 0.7 mL/min) and (b) Variation trend of k_1 , k_2 , α and R_s at 25 °C. Experimental conditions: mobile phase, N-hexane:isopropanol=90:10. The signal was monitored with a UV detector at 254 nm.

References

1. Y. Q. An, M. Chen, Q. J. Xue and W. M. Liu, *J. Colloid Interface Sci.*, 2007, **311**, 507-513.
2. H. R. Abid, H. Y. Tian, H. M. Ang, M. O. Tade, C. E. Buckley and S. B. Wang, *Chem. Eng. J.*, 2012, **187**, 415-420.
3. R. D. Arrua, A. Peristy, P. N. Nesterenko, A. Das, D. M. D'Alessandro and E. F. Hilder, *Analyst*, 2017, **142**, 517-524.
4. X. Q. Zhang, Q. Han and M. Y. Ding, *RSC Adv.*, 2015, **5**, 1043-1050.
5. C. J. Wang, L. Zhang, X. L. Li, A. J. Yu and S. S. Zhang, *Talanta*, 2020, **218**.